Does a Monsoon Climate Exist over South America?

JIAYU ZHOU* AND K.-M. LAU

Laboratory for Atmospheres, NASA/Goddard Space Flight Center, Greenbelt, Maryland

(Manuscript received 12 December 1996, in final form 3 July 1997)

ABSTRACT

The climatology and the basic state of the summertime circulation and rainfall over South America are studied using assimilation products from the data assimilation system of Goddard Earth Observing System-1 (GEOS-1) and satellite-derived rainfall. Results indicate the existence of a regional summer monsoon circulation regime induced by strong diabatic heating over the subtropical South American highland centered at the Altiplano Plateau. Sensitivity of the results to the assimilation scheme is tested by comparing that with the National Centers for Environmental Prediction (NCEP) reanalysis and with satellite rainfall estimates. Results show general agreement between the model produced rainfall anomaly and the satellite estimates, as well as consistency between the basic circulation features in the GEOS-1 and the NCEP reanalyses.

A case study of 1989–90 South American summer monsoon (SASM) reveals the following characteristics.

1) In late spring, the onset of SASM is signaled by an abrupt merging of the upper-tropospheric double westerly jets, one in the subtropics and the other in the subpolar region, into a single jet in the midlatitudes. This is followed by the establishment of a vortex to the southeast of Altiplano and occurrence of heavy precipitation over subtropical eastern Brazil.

2) During the mature phase of SASM, the heavy rainfall zone moves over the Altiplano Plateau and the southernmost Brazilian highland. The fully established SASM features are the following: (a) an enhancement of equatorial North Atlantic trade wind, which emanates from the Sahara high and crosses the equator over the South American continent; (b) a buildup of strong northwesterlies along the eastern side of the tropical Andes; and (c) development of the South Atlantic convergence zone in the southernmost position with strong convective activity. Meanwhile, the upper-tropospheric return flow emerges from an anticyclone formed over the Altiplano Plateau, crosses the equator, and sinks over northwestern Africa.

3) The withdrawal of SASM in late summer is signaled by the resplitting of the midlatitude westerly jet. At the same time, the low-level northwest monsoon flow diminishes, reducing the moisture supply and leading to the termination of heavy precipitation over the subtropical highland.

Results also show that the above-mentioned characteristics of SASM are clearly linked to the tropospheric temperature changes over the central South American highland. Sensible versus latent heating over the highland are bound to play an important role in the evolution of SASM.

To provide further support of presence of a monsoon climate over South America, SASM is compared and contrasted to the ''classic'' east Asian summer monsoon (EASM). Many similar features, including evolution characteristics between the two systems, have been identified. Contrasting aspects of the SASM from the EASM are also discussed. It is pointed out that a number of monsoonal characteristics of the climate of South America, such as the seasonal reversal of the low-level wind, become apparent only when the strong annual mean wind is removed. Based on the characteristic features and their evolution, the authors conclude that a monsoon climate does exist over South America.

1. Introduction

Monsoon climate is notable in many places around the world. In a broad sense, the term ''monsoon'' usually indicates a seasonal reversal in the large-scale circulation system driven by differential heating of the continents and the oceans. As early as the seventeenth century, Halley (1686) described the elements of a monsoon climate focusing on regions receiving an excess of solar energy and their association with the seasonal movement of the sun. He pointed out that the strength and extent of the monsoon are determined by the nature of the land, its topography, and by the excess of solar insolation. To identify the monsoon areas, Khromov (1957) proposed a monsoon index based on the change in the prevailing wind direction and its average frequency. Ramage (1971) modified Khromov's definition of a monsoon to include the measure of strength and persistence of annual wind variations. These principles in defining a monsoon have been accepted by the meteorological community worldwide (Das 1986).

According to the Khromov–Ramage definition, South

* Additional affiliation: Space Applications Corporation, Vienna, Virginia.

Corresponding author address: Dr. Jiayu Zhou, NASA/GSFC, CODE 913, Greenbelt, MD 20771.

America is monsoonless, since there is no seasonal reversal of wind direction in the lower troposphere over the region. Ramage (1971) attributed the absence of a South American monsoon to two primary reasons: 1) the narrowness of the continent away from the equator, which limits the areas in which stationary polar highs or heat lows can form, and 2) the persistent oceanic water upwelling along the west coast, which keeps sea surface temperature (SST) lower than surface air temperature of the continent all the year round. Such a notion of a monsoonless climate state in South America lasted until the recent decade when the thermal impact of the Altiplano Plateau was brought to light (Rao and Erdogan 1989).

Over subtropical South America, the Altiplano Plateau of Peru–Bolivia (15°–21°S) is well known for its vast area of some 100 000 km^2 and high elevation at about 3700–4100 m. During austral summer, a warm-core anticyclone, known as the Bolivian high, strongly develops in the upper troposphere over the plateau. Located to the east is an upper-level trough extending over the western South Atlantic. Meanwhile, a continental heat low develops at low levels in the region of the Paraguayan–Argentinean Gran Chaco and Pampean Sierras. Distinct northerly and northwesterly low-level flow evolves along the eastern slopes of the tropical and subtropical Andes and east-northeasterly trades prevail over much of the Amazon basin. Virji (1981) showed most of these characteristics of the South American summertime circulation from early observations of the cloud wind data from the geostationary satellite.

In search for a better understanding of the formation of the Bolivian high and subsequently the summer climate of subtropical South America, Schwerdtfeger (1961) raised the question, can the Bolivian high be interpreted as the consequence of ''thermal'' or of ''dynamic'' processes? Due to the lack of observations over the plateau region, Schwerdtfeger cited from traveler's logs and reports of severe thunderstorms frequently occurring over Altiplano during the summer months. He conjectured that the Bolivian high could be thermally produced and maintained by the intense sensible heating of the plateau as well as by the latent heat release in thunderstorms. Based on observed strong vertical wind shear at Antofagasta (west coast of South America, at the Tropic of Capricorn), Gutman and Schwerdtfeger (1965) estimated the heat budget for the Altiplano region. They confirmed the existence of a heat source over the plateau and its eastern slope and concluded that the Bolivian high is maintained by the latent heat released in the severe thunderstorms and to a lesser degree by the sensible heating of the atmosphere over the plateau.

Using improved data from the First GARP (Global Atmospheric Research Program) Global Experiment (FGGE), Rao and Erdogan (1989) conducted a heat budget study over the Altiplano Plateau and its vicinity for January 1979. They demonstrated that the latent heating developing in the eastern and northeastern part of the plateau is the most important contributor to the atmospheric heat source. Most impressively, their comparison of elevated heat source over Altiplano with that over Tibet showed that the heating over northeastern Altiplano (100–200 W m^{-2}) in January was stronger than that over mid- and eastern Tibet (100–120 W m^{-2}) in July of 1979. They suggested that the upper-tropospheric monsoon circulation over subtropical South America could be driven by strong summertime heating over the Altiplano Plateau.

The concept regarding the generation of Bolivian high by the heat source over the Altiplano was questioned by Silva Dias et al. (1983), who used a linear model with a single baroclinic mode to show that the Bolivian high is essentially due to the equatorial Rossby wave response to the Amazonian transient heat forcing. This study has been substantially expanded by other investigators (DeMaria 1985; Buchmann et al. 1986; Silva Dias et al. 1987; Kleeman 1989; Gandu and Geisler 1991; Figueroa et al. 1995) using different models but with similar conclusions, all pointing to the importance of the diabatic heat source over the Amazon Basin. The Andes was considered only for its dynamical effect on the disturbance generated by the Amazonian diurnal convective heating. The strong latent heating accompanying severe thunderstorm activity over the Altiplano Plateau was not considered in the above-mentioned studies.

Kalnay et al. (1986) performed a study using a general circulation model (GCM) to unravel the mechanism for the development of short-scale stationary wave activity over central South America in January 1979. The wave characteristics of the leeside ridge and the barotropic structure led them to conclude that the wave is not orographic in origin, but it is generated by the Rossby wave response to the Amazonian heating. However, the possibility that the January wave may be a response to the intensification of the Bolivian high has not been considered. Instead of focusing on the formation of the Bolivian high, Kousky and Alonso Gan (1981) aimed at the genesis of the upper-tropospheric cyclonic vortices in the tropical South Atlantic. They found a direct relationship between the occurrence of the vortices and the amplification of the Bolivian high. They speculated this relationship could be linked to the midlatitude cold frontal systems penetrating into low latitudes.

In a recent investigation, Lenters and Cook (1995) identified five climatological summertime precipitation maxima over the South American continent in January. They found that the precipitation maxima in the Amazon, South Atlantic convergence zone (SACZ), and northern Andes regions are mostly the results of low-altitude continental heating. The precipitation maxima located at the eastern flank of the central Andes (part of the center over central Andes) and the western flank of the southern Andes are introduced by the barrier effect of the mountain. Strong precipitation at high elevations of the central Andes is associated with locally

driven small-scale convergence, which may be related to the strong sensible and latent heating over the Altiplano Plateau.

Compounded by the above-mentioned uncertainties concerning the ''monsoon climate'' of South America, the role of South American summer monsoon (SASM) in the global climate is even less known. For example, whereas the Asian monsoon is known to play a significant role in interannual variability such as the El Niño–Southern Oscillation and the tropospheric biennial oscillation (Webster and Yang 1992; Meehl 1993; Shen and Lau 1995), the influences of these large-scale climate fluctuations on SASM and possible feedback mechanisms are virtually unknown. As will be shown in this paper, the SASM variability is closely linked to trade wind fluctuations over the equatorial Atlantic, which have significant impact on air–sea interaction related to ENSO as well as interannual and interdecadal SST variations over the Atlantic.

The above consideration provides the motivation of this work. In this paper, we have carried out a diagnostic study on the seasonal characteristics of the heating distribution and the associated circulation, using the reanalysis products of the data assimilation system (DAS) with version 1 of the Goddard Earth Observing System (GEOS-1) and comparing the results with the National Centers for Environment Prediction (NCEP) reanalysis and the GOES (Geostationary Operational Environmental Satellite) Precipitation Index (GPI). This paper will provide guidance for ongoing work on interannual variability of the SASM. In sections 2 and 3, we first introduce the datasets used in this study. Next, we focus on the change of thermal structure from spring to summer and its impact on the circulation regime over tropical and subtropical South America. In section 4, a case study for the period of October 1989–April 1990 is conducted to demonstrate the characteristics of monsoon evolution and the associated heating diagnostics. Section 5 is devoted to a comparison between SASM and the ''classic'' monsoon climate of the Asian summer monsoon. Section 6 presents the conclusion. More detailed comparisons in some key aspects of SASM with NCEP reanalysis and GPI rainfall estimation are included in the appendix.

2. Data

The GEOS-1 DAS reanalysis data used in this study cover the period from March 1980 to November 1993. A comprehensive description of the technical details can be found in Schubert et al. (1993). In the process of assimilation, the prognostic fields are mostly determined by a blending of observations and model dynamics, whereas the diagnostic quantities are closely related to the model's physical parameterization. Schubert and Rood (1995) showed that the basic prognostic fields provide a reasonably good agreement with the available observations in terms of climate mean and seasonal cycles. Deficiencies are found mostly tied to biases in the humidity and cloud fields, which are model and analysis scheme dependent. In the Southern Hemisphere, where observation is sparse, many uncertainties are related to the model biases. To ensure that the data are valid, we compare results from GEOS-1 DAS to the reanalysis produced by NCEP (Kalnay et al. 1996) from 1979 to 1995. Since substantial problems have been found in the rainfall assimilation in both GEOS-1 and NCEP reanalysis (Higgins et al. 1996), the GPI from 1986 to 1994 (Arkin and Meisner 1987) is used as an independent observational reference for the spatial pattern of the SASM rainfall. According to Xie and Arkin (1995), the spatial rainfall pattern of GPI rainfall is more reliable than its magnitude, especially over tropical land.

3. Heating characteristics and circulation regime

Results of this section are based on the climatology of GEOS-1 reanalysis (1980–93) and in comparison with the NCEP climatology (1979–95).

From austral spring to summer, the circulation over South America evolves in two distinct stages. In October, heavy precipitation, mostly convective type, occurs over Central America and the Amazon basin due to the strong surface heating by solar radiation (See Fig. 1a for GPI rainfall climatology). At this stage the circulation regime is strongly controlled by the equatorial dynamics (Fig. 2). Since the geostrophic relation is not valid in the deep Tropics, the wind and the pressure continually adjust to each other. Because of the weak nonlinear advective processes normally found at low latitudes, the pressure-wind adjustment can be qualitatively interpreted by the linear dynamics of individual waves (Silva Dias et al. 1983). Figures 2a and 2b show that the upper-tropospheric anticyclonic circulation center appears just above the southern edge of the Amazon basin at 8°S and 62°W in the climatology of GEOS-1 DAS and slightly farther south in that of the NCEP reanalysis, respectively.

Following the seasonal migration of the sun, the major heating zone migrates to the subtropics in summer. Here, quasigeostrophic adjustment accounts for much of the regional circulation pattern, which is forced by the large-scale diabatic heating in the subtropics. Figure 1b shows that the precipitation substantially weakens over Central America and the northwestern South America. Distinct rainfall enhancement occurs over the central Andes, southern Brazil, and the north coast of Brazil. Figure 3 displays the GEOS-1 DAS climatology of the midtropospheric thermal structure in January. Though the diagnostic fields of the reanalysis may not be quantitatively reliable, the area of the principal heating, which is southward shifted from the Amazon basin to the subtropical hilly region, is consistent with that of the precipitation enhancement depicted by GPI in Fig. 1b. The strongest heating center occurs coherently with the temperature ridge around 20°S. As a result, the eddy available potential energy is generated effectively. Fig-

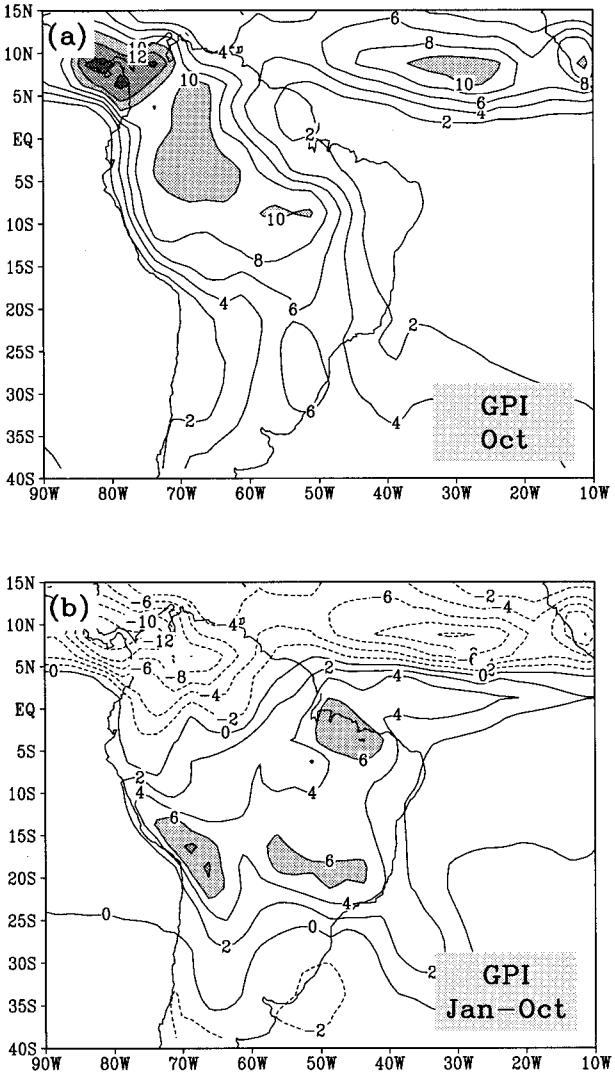

FIG. 1. GPI climatology for (a) the October mean and (b) the difference of January minus October. Unit: mm day^{-1}.

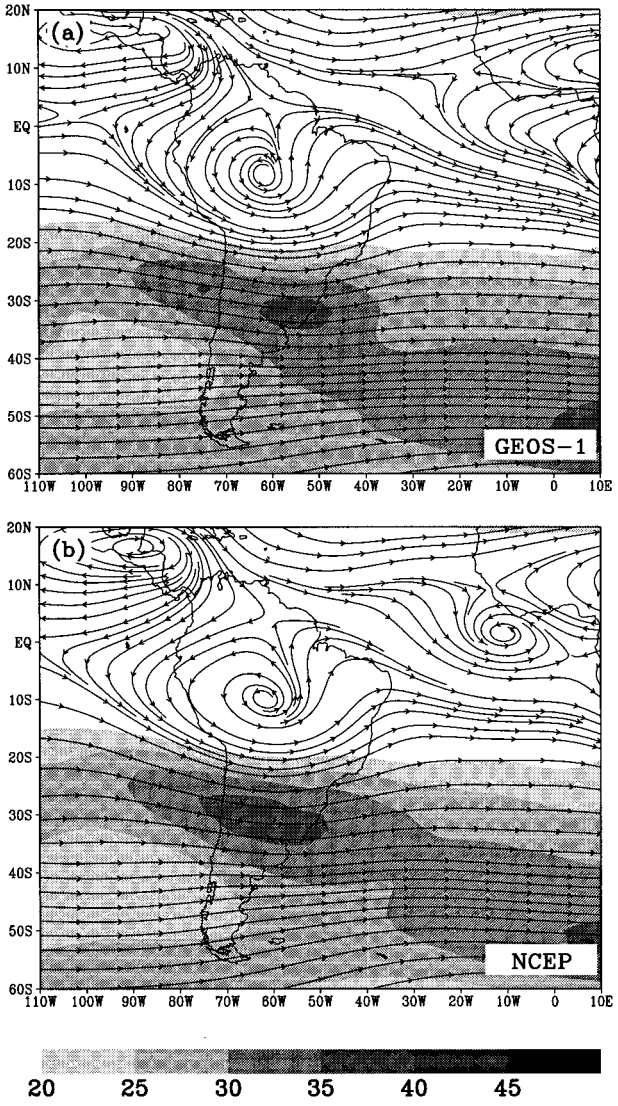

FIG. 2. Climatology of the October mean 200-hPa streamline for (a) GEOS-1 DAS and (b) NCEP reanalysis. The shading indicates wind speed (m s^{-1}).

ure 4 shows significant rising motions accompanied with available potential energy release over the Altiplano Plateau and southern Brazil with low-level convergence and upper-level divergence. At the same time, the rising center of the previous season, over the Amazon basin around 6°S, has weakened substantially. The monsoonal circulation regime is ultimately formed by transforming energy from the divergent to the rotational circulation. In the upper troposphere, the anticyclonic center moves onto the Altiplano Plateau, 10° south and 3° west of the former position in October in both GEOS-1 DAS and NCEP reanalysis (see Fig. 5). On the eastern side of the center, distinct south-southeasterlies develop, which turn toward the Subsaharan zone after crossing the equator. At the low levels, the north-northwesterly flow intensifies along the eastern slope of the subtropical Andes and turns cyclonically over Gran Chaco (20°–30°S). This feature was also described by Virji (1981), who used the data derived from satellite observation and showed that the speed of the low-level north-northwesterly cloud wind in that region can reach as high as 25 m s^{-1} on individual days in the southern summertime. The vertical wind shear over the monsoon region is governed by the thermal wind relation in the presence of a horizontal temperature gradient. Figure 6 shows the vertical cross section of January meridional wind along 20°S. Strong vertical shear of the meridional wind over both sides of the plateau represents a baroclinic character, which is in agreement with the temperature contrast between the subtropical South American continent centered in the Altiplano Plateau and its surrounding ocean. These features are captured by both the GEOS-1 and NCEP reanalyses.

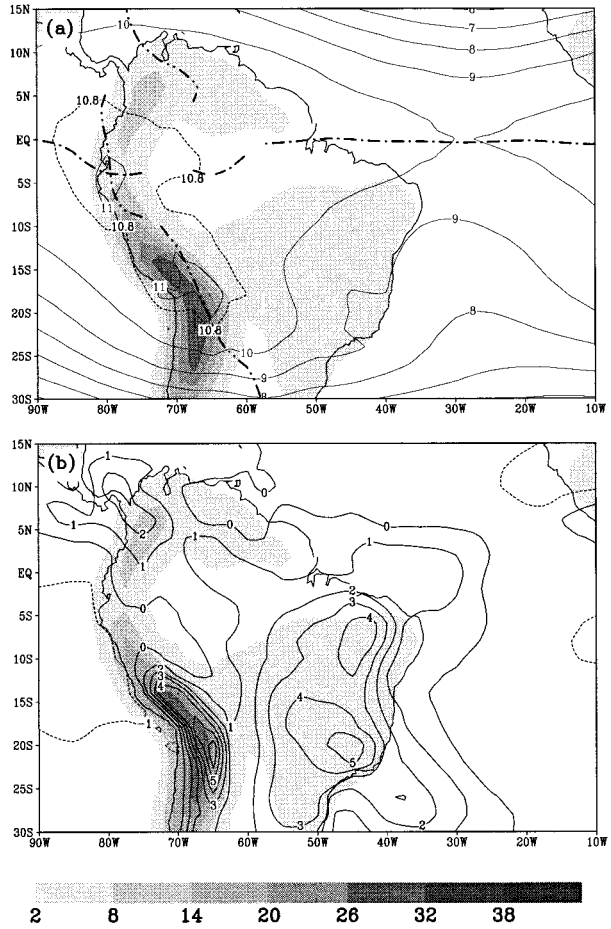

FIG. 3. GEOS-1 DAS climatology of the January mean 400-hPa (a) temperature (K) and (b) total diabatic heating (K day^{-1}). The global means have been subtracted for both fields. The dash-dotted lines indicate the temperature ridge and shadings the orography (hm).

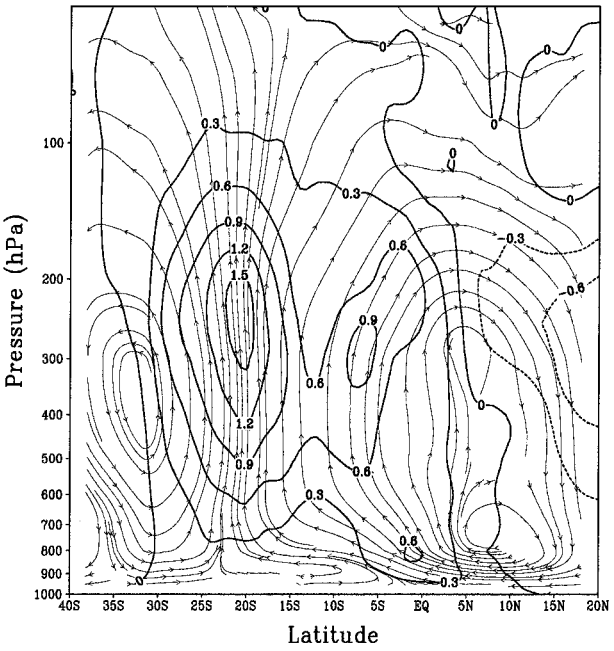

FIG. 4. GEOS-1 DAS climatology of January mean 65°–40°W zonally averaged meridional circulation. Contours indicate the vertical velocity (cm s^{-1}) and arrow lines the streamline.

Along with the seasonal change of the heating pattern, the air mass is redistributed. Figure 7 shows that from early spring to midsummer, a low pressure system develops over Gran Chaco, reaching its strongest in December and January. Meanwhile, pressure increases substantially over the northwestern Sahara. As a result, the cross-equatorial pressure gradient from the southwest to the northeast strengthens and the cross-equatorial flow develops. Figures 8a and 8b show the vertical structure of the meridional wind along the equator in January for GEOS-1 DAS and NCEP reanalysis, respectively. Overall, NCEP reanalysis displays more intense cross-equatorial flows in both the upper and lower troposphere than the GEOS-1 DAS assimilation, which is consistent with the finding of a much stronger Hadley cell in the NCEP reanalysis by Schubert and Rood (1995) and Higgins et al. (1996). In the low level, both reanalyses agree that the core axis of the maximum northerly is located below 800 hPa and inclines eastward. In the upper level, strong southerlies centered around 45°W at 150 hPa are found in both reanalyses, but the further westward extension of the southerlies as being apparent in the NCEP reanalysis has no counterpart in the GEOS-1 DAS assimilation.

Halley (1686) defined monsoon as a large perturbation on the general trade winds of the Tropics. Over the tropical Atlantic, the seasonal reversal of the surface wind is not readily apparent because the easterly trade winds prevail all year round (see Fig. 9a). However, when the annual mean component is removed, the seasonal reversal in surface wind is quite obvious. Figures 9b and 9c show, respectively, the GEOS-1 DAS climatology of January and July 900-hPa wind anomaly in which the annual mean has been subtracted. In the Southern Hemisphere summer, the anomaly flow originates from the Subsaharan region and substantially enhances the tropical North Atlantic easterly trades. After crossing the equator, it becomes a northwesterly flow along the eastern side of the Andes, then turns clockwise around the low of Gran Chaco. Clearly, this flow reverses its direction in southern winter. The above noted wind reversal, which is also found in the NCEP reanalysis (see appendix), is one of the many factors vouching for the presence of a monsoon climate in South America.

4. 1989–90 South American summer monsoon

To demonstrate more detailed temporal evolution of SASM, 10-day mean data are constructed for the period from August 1989 to April 1990. This period corresponds to near-normal tropical SST and represents a

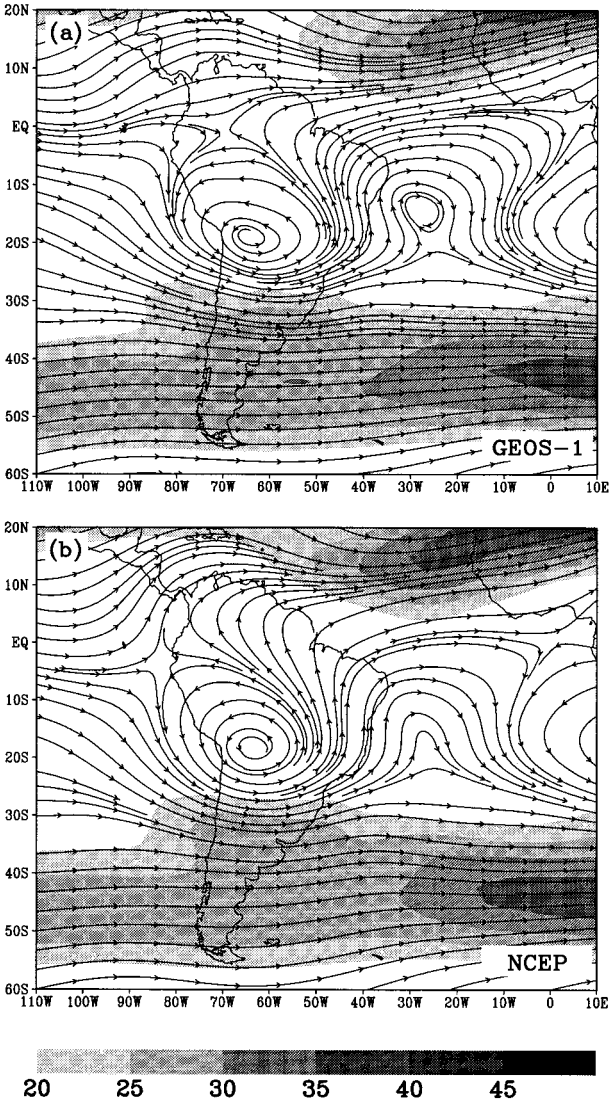

FIG. 5. Same as Fig. 2 except for January.

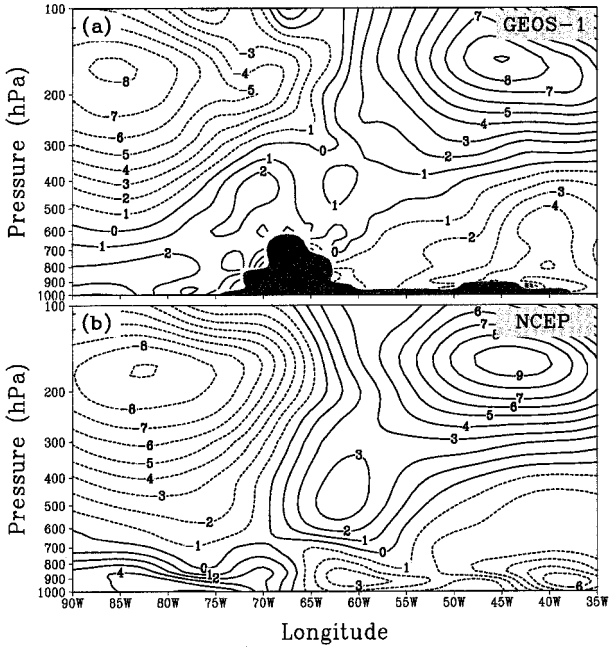

FIG. 6. Vertical cross section of the January mean climatology of the meridional wind (m s^{-1}) along 20°S latitude for (a) GEOS-1 DAS and (b) NCEP reanalysis.

typical normal year, when the influence of interannual variability is relatively small.

a. Abrupt phase change

According to van Loon (1972), the Southern Hemispheric westerly wind field is characterized by a single maximum in summer and double maximum in winter, except over South America where a single jet is maintained in both seasons. Figure 10a exhibits the seasonal migration of 200-hPa westerly jet axis over the South American continent. From September to October, the upper-tropospheric zonal wind exhibits a double maximum, one over the subtropics (30°S) and the other over the subpolar region (56°S). Around the middle 10 days of November, an abrupt change occurs. The westerlies suddenly strengthen in midlatitudes and weaken in lower and higher latitudes, resulting in a single jet stream around 46°S, which prevails throughout the subsequent two months. From March to April, the westerly jet system switches back to a double maximum. This period lasts about one month until the seasonal transition is finally completed in April when the single maximum reappears.

The time evolutions of heavy precipitation activity over the western high mountain range and the eastern low land are presented in Figs. 10b and 10c, respectively. Accompanying the sudden merge of the double westerly jet in late spring, heavy precipitation occurs abruptly at 18°S over the east and 15°S over the west. The figures show that the poleward migration of the strong convective activities over the eastern side of the continent leads that over the western side, and both movings are in stepwise manner. During December and January, when the westerlies have a single maximum, two stages can be distinguished as evident in the abrupt poleward jump of the heavy precipitation center around the end of December. In the middle of February, heavy precipitation in the subtropics terminates at about the same time the westerly jet split into two cores.

Based on the timing of the abrupt change of the circulation and the precipitation pattern, five phases (see Table 1) can be identified. To elucidate the characteristic features of SASM for each phase, a composite analysis has been carried out.

b. Phase composite

The time evolution of 200-hPa and that of 850-hPa wind composites are displayed in Figs. 11 and 12, re-

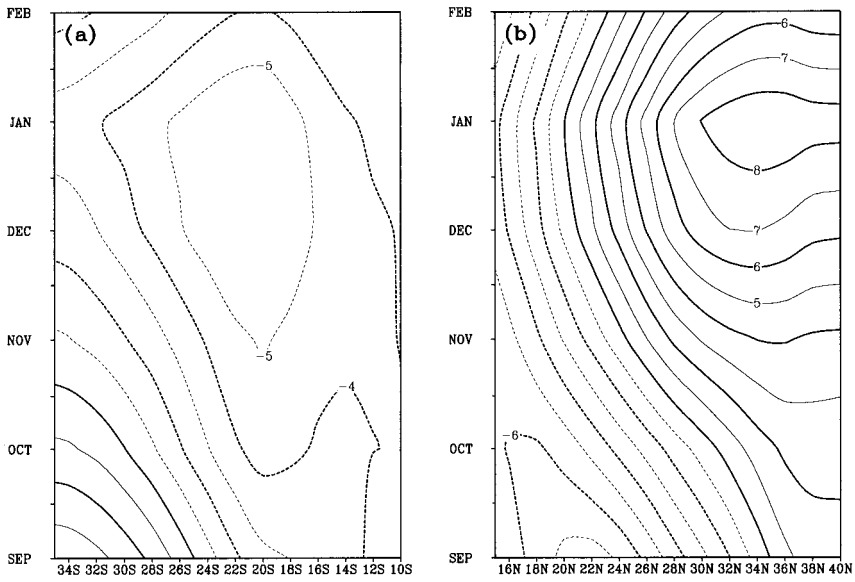

FIG. 7. GEOS-1 DAS climatology of the evolution of the monthly mean sea level pressure (hPa), zonally averaged (a) from 65° to 50°W and (b) from 10°W to 10°E. The mean value of the domain (90°W–20°E and 40°S–40°N) has been subtracted for each month.

spectively. The composite precipitation difference between two consecutive phases is shown in Fig. 13. In the premonsoon period (phase I), the centers of the upper-level divergence (Fig. 11a), and the lower-level convergence (Fig. 12a) are situated above the Amazon basin. This arises as a result of local strong convective heating. In the subtropical region, upper-tropospheric westerly wind is strong, and low-level easterly winds flow from the tropical and subtropical South Atlantic to the foot of the northern Andes. The strong vertical shear indicates that temperature contrast between the Tropics and extratropics is dominant at this stage.

During phase II, the summer monsoon develops with vigorous low-level cyclonic activity to the southeast of Altiplano (Fig. 12b). The equatorial trade winds over the North Atlantic enhance and cross the equator upon reaching the Andes, forming a strong northwest to southeast low-level flow along the southwestern bound-

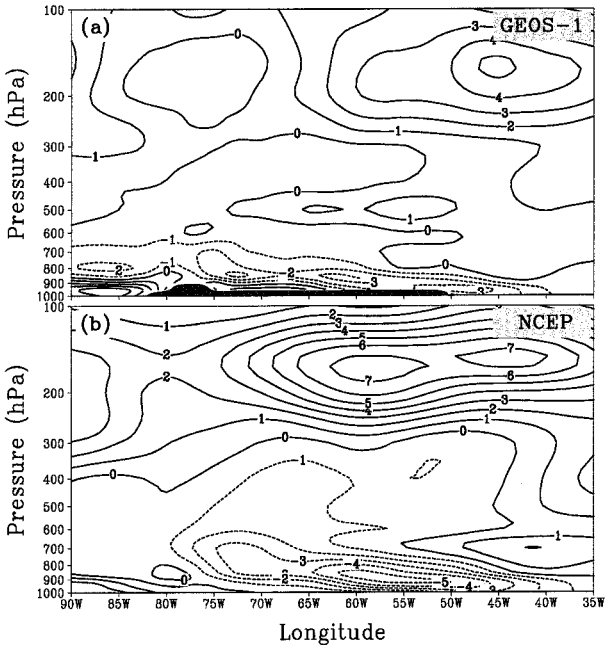

FIG. 8. Same as Fig. 6 except along the equator.

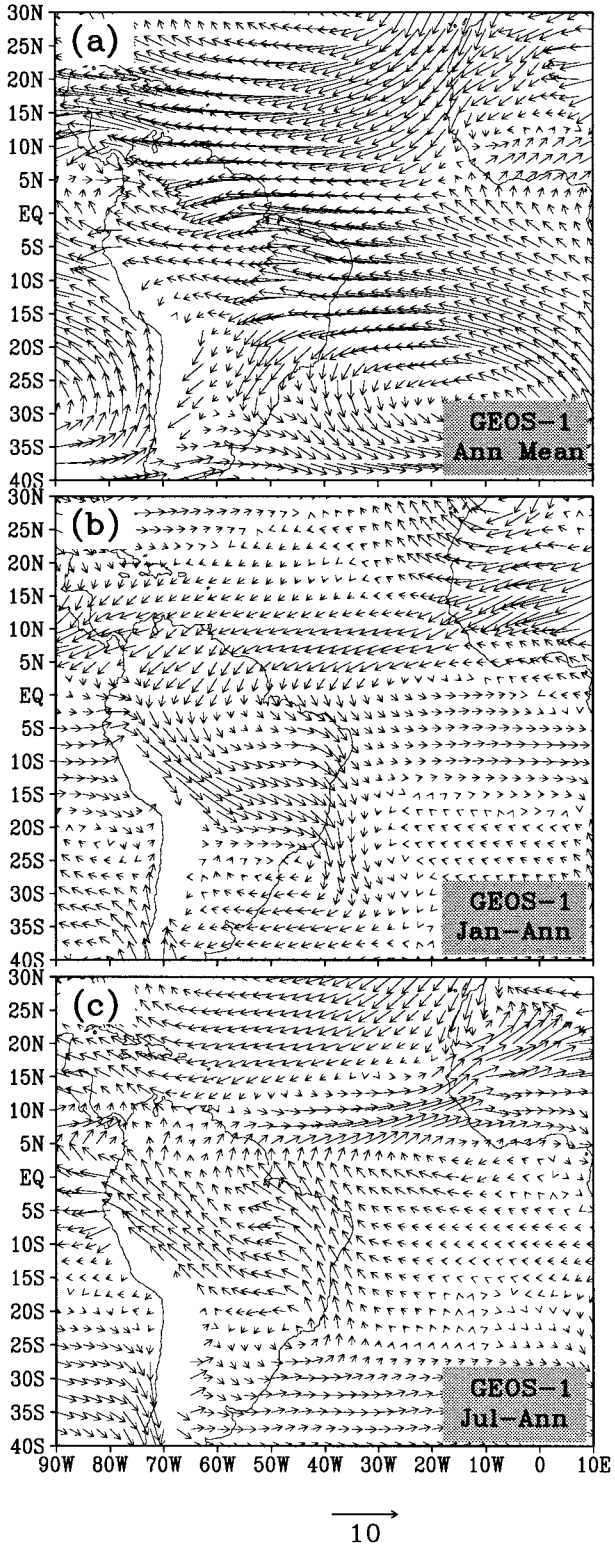

FIG. 9. GEOS-1 DAS climatology of 900-hPa wind (m s^{-1}) for (a) annual mean, (b) January minus annual mean, and (c) July minus annual mean.

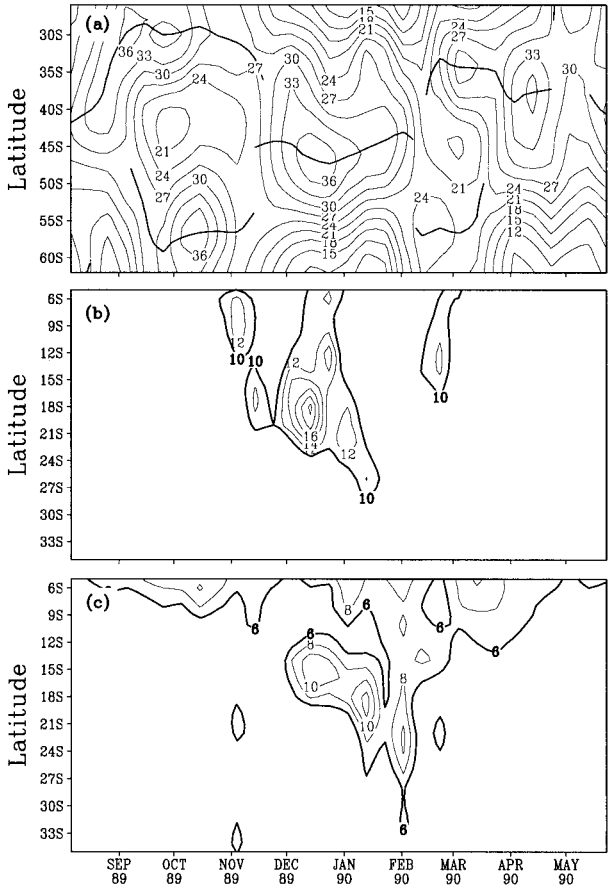

FIG. 10. Latitude–time section of GEOS-1 assimilation of (a) 200-hPa zonal wind speed (m s^{-1}), zonally averaged from 75° to 45°W; (b) heavy precipitation (mm day^{-1}), zonally averaged from 68° to 63°W; (c) same as (b) but from 55° to 43°W. The bold lines in (a) show the migration of the westerly jet axis.

ary of the Amazon basin. Meanwhile, the anticyclonic center in the South Atlantic moves toward the continent. The phase difference of the precipitation field shows a southeastward movement of the heavy rainfall center from phase I to phase II (Fig. 13a). The rainfall amount increases over the central Andes, but the most severe thunderstorms are initiated over southeastern Brazil, which may be connected to the activation of SACZ. Simultaneously, the upper-tropospheric circulation experiences substantial strengthening of the anticyclone over the southern Amazon basin and deepening of the trough over the subtropical western South Atlantic

TABLE 1. Phase partition of 1989–90 South American summer monsoon.

Period	Phase	Description
1 Oct–19 Nov 1989	I	Premonsoon
20 Nov–29 Dec 1989	II	Monsoon development
30 Dec 1989–7 Feb 1990	III	Monsoon mature
8 Feb–19 Mar 1990	IV	Monsoon withdrawal
20 Mar–28 Apr 1990	V	Postmonsoon

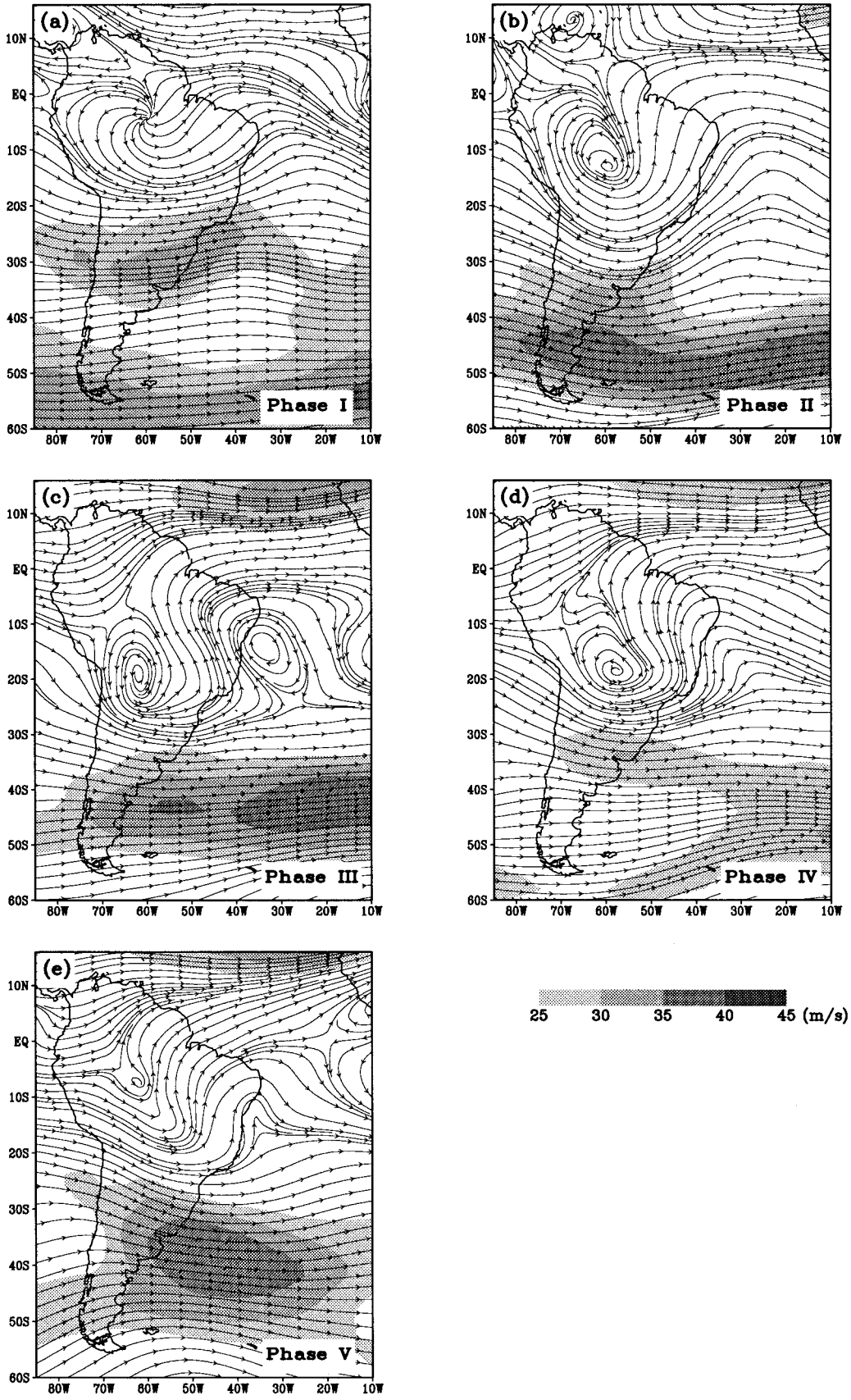
(a)
Phase I
(b)
Phase II
(c)
Phase III
(d)
Phase IV
(e)
Phase V
10N
EQ
10S
20S
30S
40S
50S
60S
80W
70W
60W
50W
40W
30W
20W
10W
25
30
35
40
45 (m/s)

Ocean (Fig. 11b). The development of meridional circulation on the eastern side of the continent indicates a large increase of the influence of the thermal contrast between the central South American continent and the subtropical western South Atlantic Ocean.

In phase III SASM enters the mature stage. At this stage the heavy precipitation center embedded in the SACZ migrates farther southwestward to the southernmost position (about 26°S). The rainfall over the subtropical Andes is substantially intensified (Fig. 13b). As evident in Fig. 11c two closed circulations, the Bolivian high and the South Atlantic low, are formed in the upper troposphere. Between the two gyres, low-level northerlies and high-level southerlies prevail, showing remarkable thermal wind relation, which prompts the warm center developing over the Altiplano Plateau.

During phase IV, the SASM starts to withdraw. As shown in Fig. 10a, the withdrawal signal can be clearly identified by the resplitting of upper-tropospheric westerly jet. During this period, the cross-equatorial flow weakens. Due to the reduction of moisture supply to the subtropics, the major precipitation center retreats northeastward from the subtropics (Fig. 13d). As a result, the differential heating between the subtropical continent and the adjacent ocean becomes insignificant (discussed in the next section) and no longer supports the vertical wind shear over the monsoon region. On the eastern side of the tropical Andes, the low-level northwesterly monsoon flow is broken (Fig. 12d). At the high level, the Atlantic low deteriorates into a trough, and the Altiplano anticyclone weakens and shifts away from the plateau (Fig. 11d).

During phase V, the postmonsoon circulation regime is built up, characterized by a uniform upper-tropospheric westerly jet stream at about 35°–40°S. Much of the rainfall returns to the Tropics as a result of the low-level moisture convergence by the trade wind. Large-scale wave response to the Amazonian heating can be clearly seen from the 200-hPa wind field (Fig. 11e), which shows a ridge-trough system tilting from the northwest to the southeast in the east of the Andes.

c. Temperature and heating evolution

The evolution of the monsoon circulation described above is linked to the tropospheric temperature change over the subtropics. Figure 14a shows the time evolution of the mean tropospheric temperature (200–600-hPa averaged) over the subtropical domain (26°–16°S). To highlight the relative warming and cooling, the annual mean of the spatial domain average is removed. From the middle of October to the end of April, temperature over the subtropical highland oscillates with a period of about 40 days, which coincides with the phases defined in the previous section. The tropospheric warming starts over the central Andes from the end of October (phase I). Temperature increases in association with the monsoon onset. From the middle of November to the middle of December, tropospheric temperature increases more than 3 K in the east of the central Andes. Warm air first expands eastward, reaching around 40°W, then spreads westward, getting as far as 100°W in the end of December. At the same time, the relatively cold air evolves over the subtropical South Atlantic Ocean. The sharpest east–west temperature contrast of about 7 K between the warm and the cold centers is maintained in the middle of December (phase II), the time of the strongest monsoon development. In the mature stage (phase III), the warm center moves onto the plateau and the eastern cold center weakens. The warm air is most widespread in early January. It shows clearly that the time period of phase II and III lasts about 2.5 months with intense warming over the subtropical hilly continent of more than 3 K above the spatial and temporal mean value. During this period the upper-tropospheric westerly wind maintains a single jet stream at 46°S as described in the previous subsection. The monsoon retreats (phase IV) when the warm center over the subtropical continent weakens and the temperature gradient on the eastern side of the plateau relaxes. In the end of April, the warm air withdraws from the plateau and the circulation switches to the winter regime.

Our study reveals that the tropospheric temperature oscillation is closely related to the convective activities over the subtropical region. Figure 14b shows the time evolution of 100- and 300-hPa temperature with annual mean removed and domain averaged over 65°–40°W and 26°–16°S. The figure clearly shows an inverse relationship between the variations of the two temperatures. This distinct feature was also found by Joshi et al. (1990) over the eastern Tibetan Plateau during the period of 1979 Asian summer monsoon. The inverse relationship reflects the vertical movement of the tropopause (located around 200 hPa) as a result of the convective activity in the troposphere. We can see that the temperature rises about 5 K and drops almost 7 K at the 300- and 100-hPa levels, respectively, from October to the middle of December, an indication of strong development of deep convection from premonsoon to monsoon onset. After onset, the convective activity remains at a high level and oscillates in-phase with the change of the tropospheric temperature, which can be confirmed by comparing with Fig. 14a. From the middle of April to the end of May, 300-hPa (100) temperature falls (rises) sharply, indicating significant weakening of

←

FIG. 11. GEOS-1 assimilation of 200-hPa circulation composite for different phases of the SASM: (a) premonsoon, (b) monsoon development, (c) mature stage, (d) monsoon withdraw, and (e) postmonsoon. The shading indicates wind speed in units of m s^{-1}.

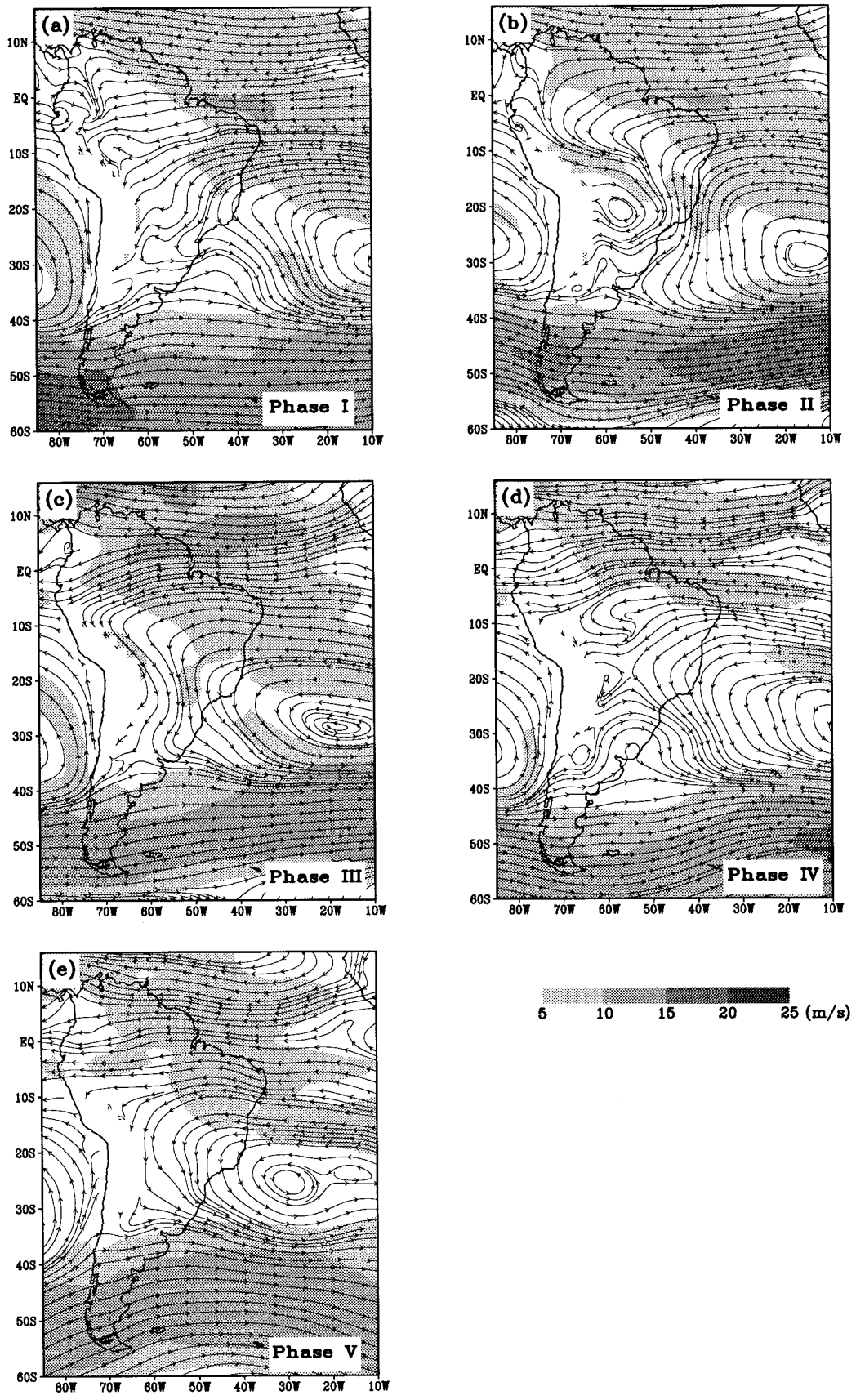

FIG. 12. Same as Fig. 11 except for 850-hPa circulation.

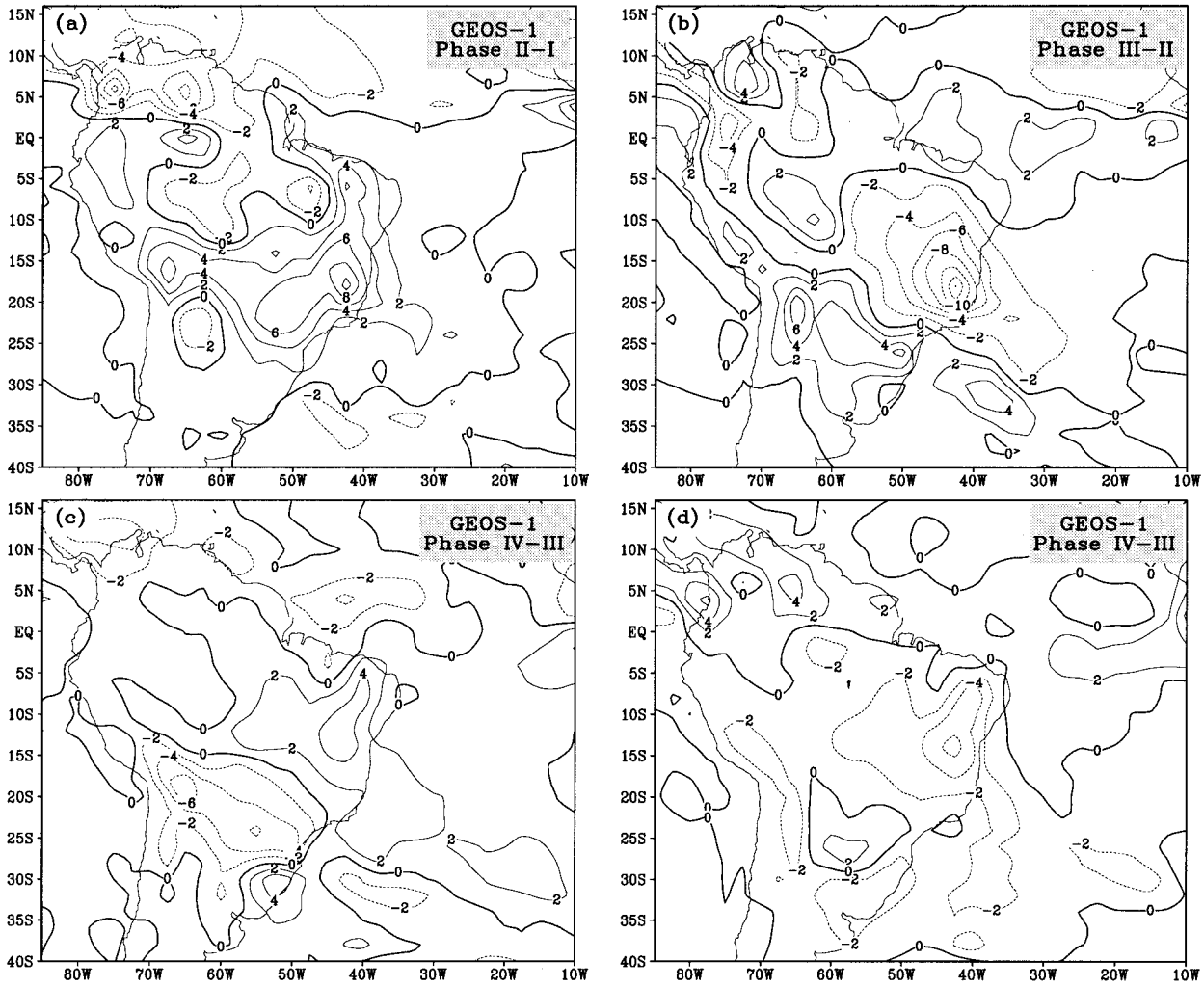

FIG. 13. Phase difference of GEOS-1 assimilated precipitation (mm day^{-1}): (a) phases II–I, (b) phases III–II, (c) phases IV–III, and (d) phases V–IV.

convective activities and cessation of heavy precipitation over the subtropical region.

Next, the vertical structure of the heating in relation to the temperature evolution is analyzed. For economy of space, only the composite pictures for phases I–III are shown in Figs. 15–17. Overall, the pictures of (a) and (b), the temperature deviation from the local zonal mean and the total diabatic heating, clearly show that the warmer area coincides with the heat source region over the subtropical continent (26°–16°S averaged), indicating the dominant role of diabatic heating in the subtropics of summertime. During phase I, significant warming starts from the low level over the plateau. Figure 15c reveals that strong heating over the plateau under 500 hPa is mainly due to the intense turbulent sensible heating induced by increasing surface temperature as a result of increasing solar energy received by the ground and vertically distributed by dry convection. Accompanying the monsoon onset, the deep convective precipitation develops over southeastern Brazil and the Altiplano Plateau (Fig. 16d), which is consistent with the analysis of Fig. 14b. The latent heat release from the deep cumulus convection becomes dominant. A midtropospheric warm core is formed in the region of the intense heating (Fig. 16a), largely increasing the thermal contrast between the continent and the nearby oceans. Turbulent sensible heating above the plateau is suppressed due to decrease of the surface temperature caused by the moistening of the ground (Fig. 16c). In the mature phase III, the strength of the heating over the continent is the strongest (Fig. 17b). The major convective heating center moves onto the plateau (Fig. 17d) with significant enhancement of the east–west circulation of the divergent wind (not shown). Adiabatic warming caused by intense subsidence over the oceans may result in widespread zonal extension of the warm area shown in Fig. 14a. In both phase II and III, the radiative cooling compensates part of the latent heating under the

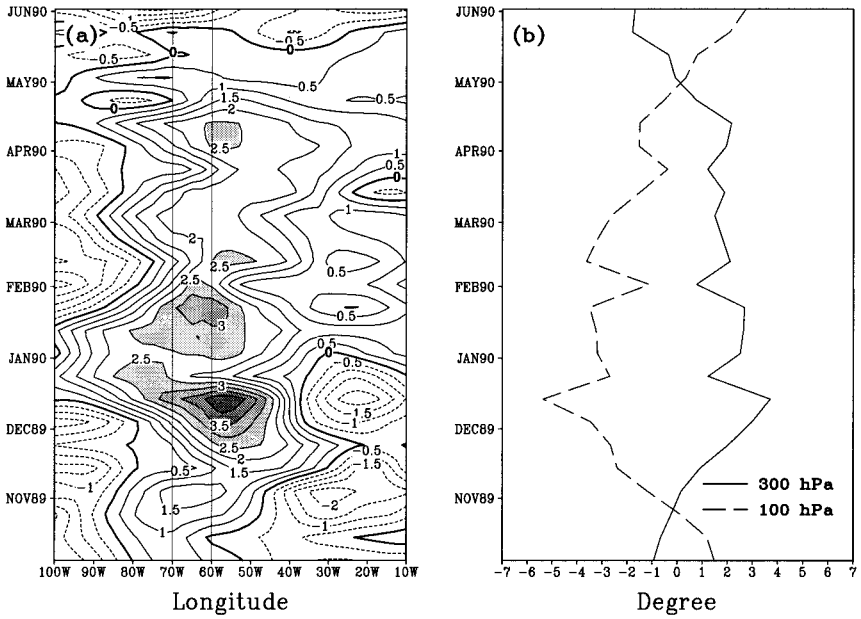

FIG. 14. (a) Time evolution of 200–600-hPa mean and 26°–16°S averaged temperature (K), with the annual mean and the domain average removed. The vertical thin lines indicate the east–west boundaries of the central Andes. (b) Corresponding time variation of 300- and 100-mb temperature over the area averaged from 65° to 40°W and 26° to 16°S. The annual mean has been subtracted.

level of 500 hPa (not shown), leading to an upward shift of the total heating profile from the latent heating profile. This feature is in agreement with Yanai et al. (1973), who found that the separation of the levels of maxima between the apparent heat source and the moisture sink profiles is a phenomenon typical for a cumulus convective atmosphere over the eastern part of the Tibetan Plateau during the Asian summer monsoon season. Accompanying the withdrawal of SASM (phases IV and V, not shown), the intensity of the convective heating drops drastically in both heating centers, which are further combined and move away from the plateau when stepping into the winter regime. The above analysis shows that the diagnostic heating field, which may not be overall reliable, can provide dynamically consistent information, which sheds light on the mechanism maintaining the monsoon circulation.

5. Comparison with East Asian summer monsoon

To provide further support of the presence of a monsoon climate over South America, it is worthwhile to compare and contrast the SASM climate as documented here to the classic monsoon climate of the Asian summer monsoon. There were several related studies (Rao and Erdogan 1989; Kodama 1992) dealing with one or two features of the two monsoon systems. Here we note that a comparison between monsoon systems should not rely on a definition based only on one or two features, but should more appropriately be in terms of all (to the extent possible) components within each monsoon system. In the following, we provide a comparison between the SASM and the east Asian summer monsoon (EASM). The later is a well-recognized monsoon system.

The importance of the land–sea distribution and orography such as the Tibetan Plateau in determining the monsoon circulation and rainfall distribution has been emphasized by many observational and GCM studies (Hahn and Manabe 1975; Druyan 1981; Ye 1981; Luo and Yanai 1984; Fennessy et al. 1994; Zhou et al. 1996). Both South America and east Asia (east of 100°E) are bordered by oceans in the east, with poleward-flowing warm currents along the coast, flanked by plateaus in the west with hilly lands in between. On the equatorward side, SASM encompasses the tropical rainforest of the Amazon basin and the EASM embraces the warm water of the South China Sea. Insofar as their influences on the overlaying atmosphere, the two regions similarly provide a warm and moist environment for major monsoon activities further poleward. Therefore, it should not be a surprise that the subcomponents of SASM could have its counterparts in EASM with similar characteristics of circulation and rainfall due to the similarity of the lower boundary conditions.

Based on the discussion in section 4, the essential features (with numbered labels) of the SASM are schematically presented in Fig. 18a. Here, we point out that the low-level monsoon flow (indicated by the thin line from northwest Africa to Gran Chaco) is considered a

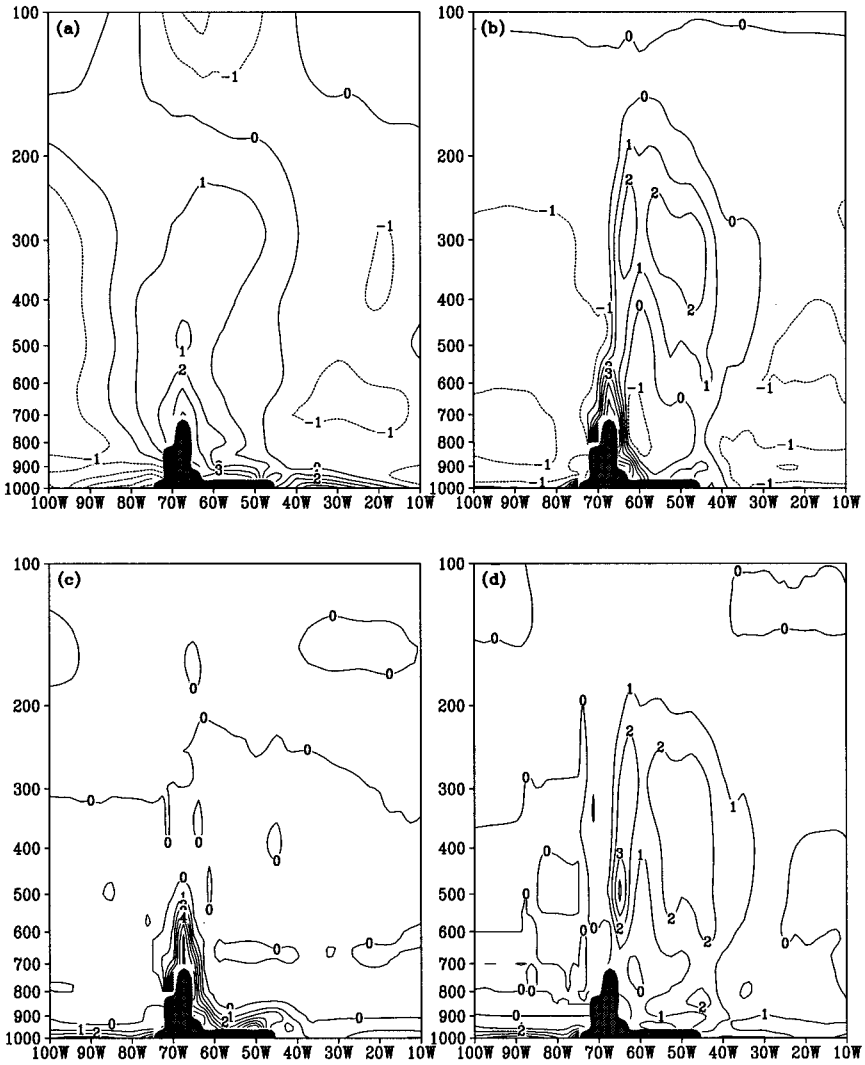

FIG. 15. GEOS-1 assimilation of phase I composite of (a) temperature deviation from the local zonal mean (100°–10°W averaged), (b) total diabatic heating, (c) turbulent sensible heating, and (d) latent heating, latitudinally averaged from 26° to 16°S. Unit: K for (a) and K day^{-1} for (b)–(d).

deviation from the annual mean tropical easterly trade wind (dashed lines). The low-level features depicted in Fig. 18a become more apparent only after the annual mean easterlies are first removed from the analysis. The large circulation features for EASM have also been computed (not shown), and a similar schematic picture for the EASM is displayed in Fig. 18b with correspondingly numbered features. The schematics in Fig. 18 represent, to our best effort, an attempt to capture features that are common to both the GEOS-1 and the NCEP reanalysis as well as the GPI rainfall estimation. The SASM low-level flow can be traced to the cold continental high of the winter hemisphere (Saharan high), which corresponds to one component of the low-level EASM flow originating from the northern Australian high. These low-level flows cross the equator, 1, and circulate cyclonically around subtropical heat lows of the summer hemisphere [Gran Chaco low, 3, vs EASM trough, 3(EAS)]. Over subtropical South America, the low-level flow is characterized by the north-northwesterlies, 2, along the eastern foothills of the tropical and subtropical Andes; the northerlies along the western edge of the South Atlantic subtropical high, 4; and the midlatitude west-southwesterlies, 6, at the south, forming a large-scale convergence zone, SACZ, 5, in the middle area. Over east Asia, southwesterly wind of Indian summer monsoon [2(IND)] and that along the western periphery of the North Pacific subtropical high, 4, encounter the midlatitude westerlies, 6, in the Yangtze valley, creating the Meiyu–Baiu frontal zone, 5, which extends from central China to Japan. Heavy precipitation associated with the cyclonic activities occurs within those low pressure systems [3 vs 3(EAS), 5]. In the upper troposphere, both monsoon systems display an anticyclonic circu-

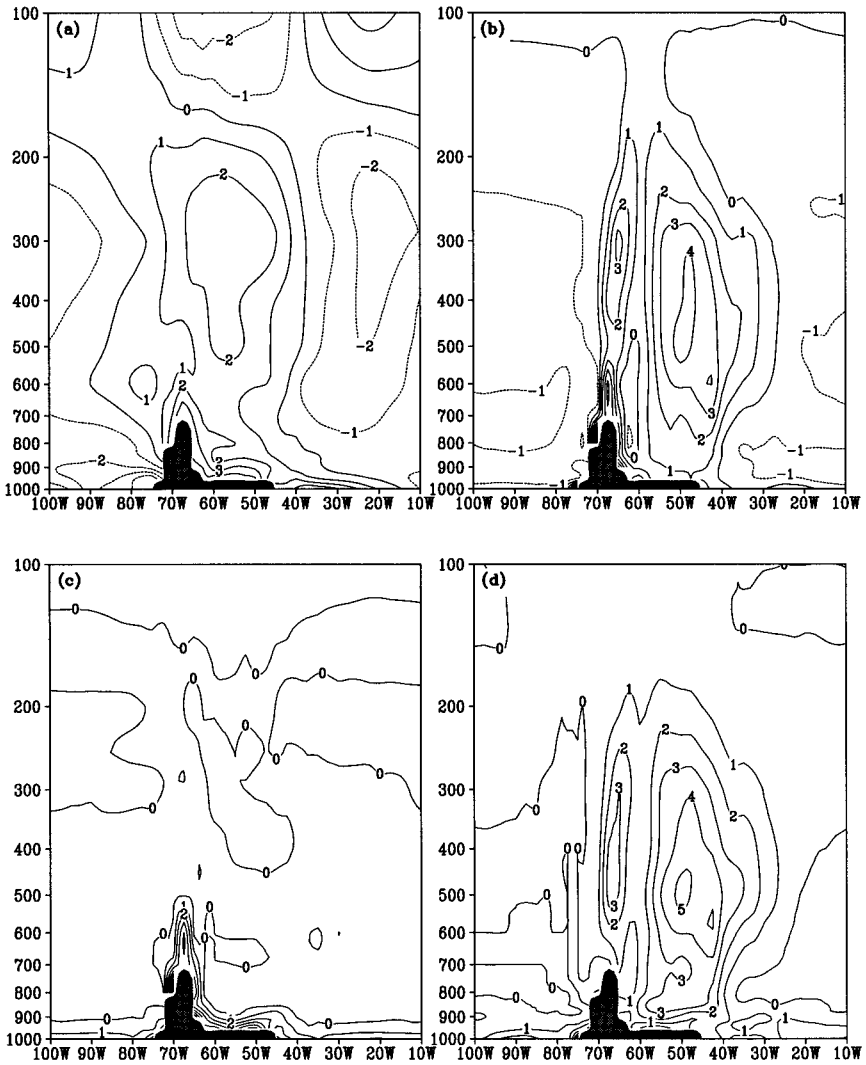

FIG. 16. Same as Fig. 15 except for the period of phase II.

lation, 7, over the plateau region. On the outskirts of the anticyclone, the return flow, 8, crosses the equator in the opposite direction of the underlying flow.

In addition to having common large-scale features SASM and EASM also evolve similarly. In section 4, we showed that the development of SASM is characterized by an abrupt enhancement of westerlies in the midlatitudes followed by stepwise poleward advances of heavy precipitation. Our results also revealed a phase lock of about 40 days in relation to the active and break cycle of the subtropical convective activity during the summer monsoon season. This may reflect the low-frequency variability within SASM and/or the far-field influence of the Madden–Julian-type oscillations. The diagnosis of the heating process demonstrated the important role played by the sensible heating over the Altiplano Plateau in early warming of the midtroposphere and the subsequent development of SASM and by the latent heat release from the strong convective precipitation after SASM onset. All these can be compared to similar monsoon features endemic to the EASM system. These features have been well documented by many investigators (Krishnamurti and Subrahmanyam 1982; Lau and Li 1984; Tao and Chen 1987; He et al. 1987; Ding 1994).

Obviously, the two monsoon systems have their differences. Although the heating over the Altiplano Plateau may be at times stronger than that of the Tibetan Plateau according to Rao and Erdogan (1989), the SASM is weaker in strength and has a shorter life span of about 2½ months (December through mid-February as seen in our case study), compared to that of the 4–5 months (May through mid-September) of EASM. This can be attributed not only to the much smaller size and lower altitude of the Altiplano Plateau but also to its lower-latitude location (20°S in EASM vs 30°S in SASM), causing the reduction of the efficiency of vorticity generation by horizontal divergence. Distinct dif-

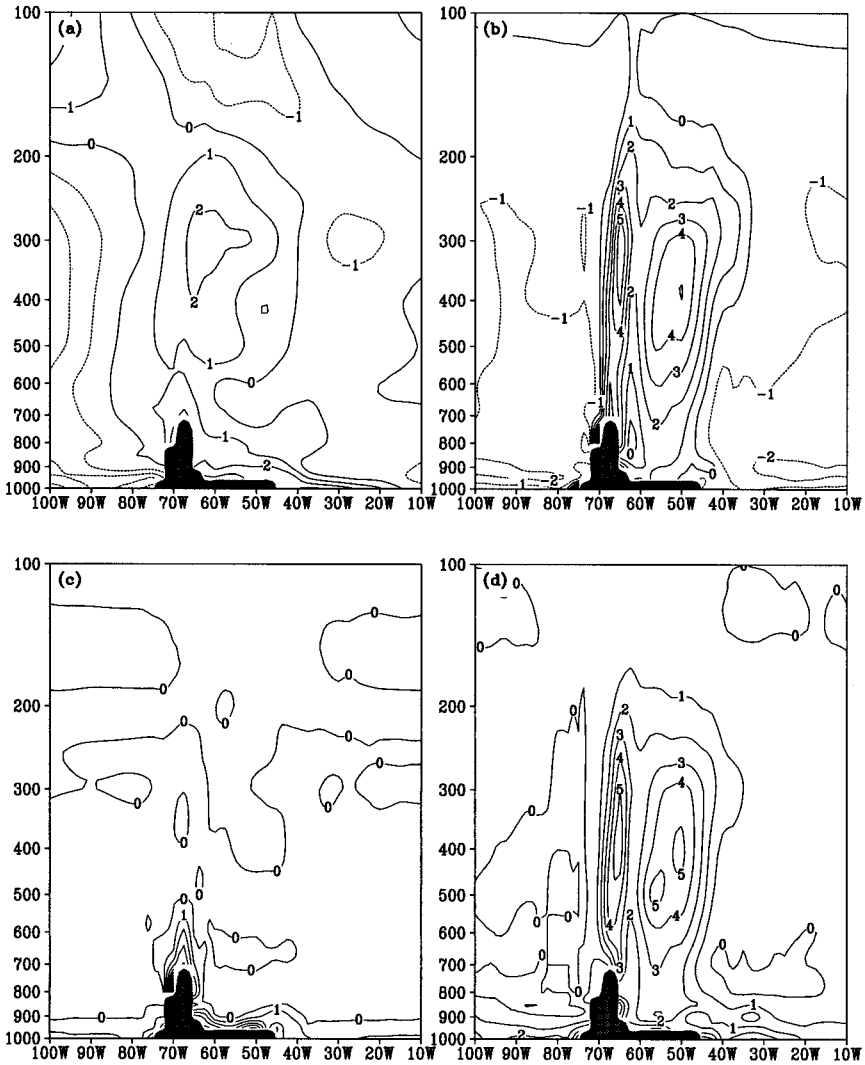

FIG. 17. Same as Fig. 15 except for the period of phase III.

ference is also found in the surface condition on the west side of two systems, that is, cold pool of the eastern South Pacific versus strong sea–land thermal contrast between South Asia and the Indian Ocean. EASM is significantly influenced by the Indian summer monsoon, which is characterized by strong surface southwesterlies and upper-level easterly jet over the Indian subcontinent as seen in Fig. 18b, whereas SASM has relatively stable circulation on its west side with prevailing subsidence all year round. Another important difference between SASM and EASM is the mechanical effect produced by the disparate shapes of the Andes and the Tibetan Plateau and their location relative to the prevailing monsoon flow. The Tibetan Plateau forces low-level monsoon westerlies to flow around the foothills of the Tibetan Plateau and over India, preventing direct north–south communication between the Tropics and midlatitudes. As a result, edge wave–like features and cyclonic development are concentrated on regions east of the Tibetan Plateau and downstream of the low-level westerlies. Whereas for the SASM, the Andes block and deflect the low-level easterlies from the equatorial Atlantic Ocean, guiding the flow toward the low of Gran Chaco. Further, they appear to cut off the influence of the Pacific Ocean, effectively shielding the west coast of South America from the direct influence of SASM.

Besides the similarities and the differences discussed above, there are some marked features of EASM that are unknown to SASM. For example, oscillations with quasi-biweekly (15–20 days) periodicities are prevalent in the Asian summer monsoon (e.g., Krishnamurti and Bahlme 1976; Lau et al. 1988). Whether similar oscillations occur in SASM cannot be diagnosed in the present study. Higher temporal resolution (at least daily) is required. Another feature is that the EASM is known to play an active role in ENSO and in tropospheric biennial oscillation (Lau 1992; Meehl 1993). What role, if any, the SASM plays in these important climatic

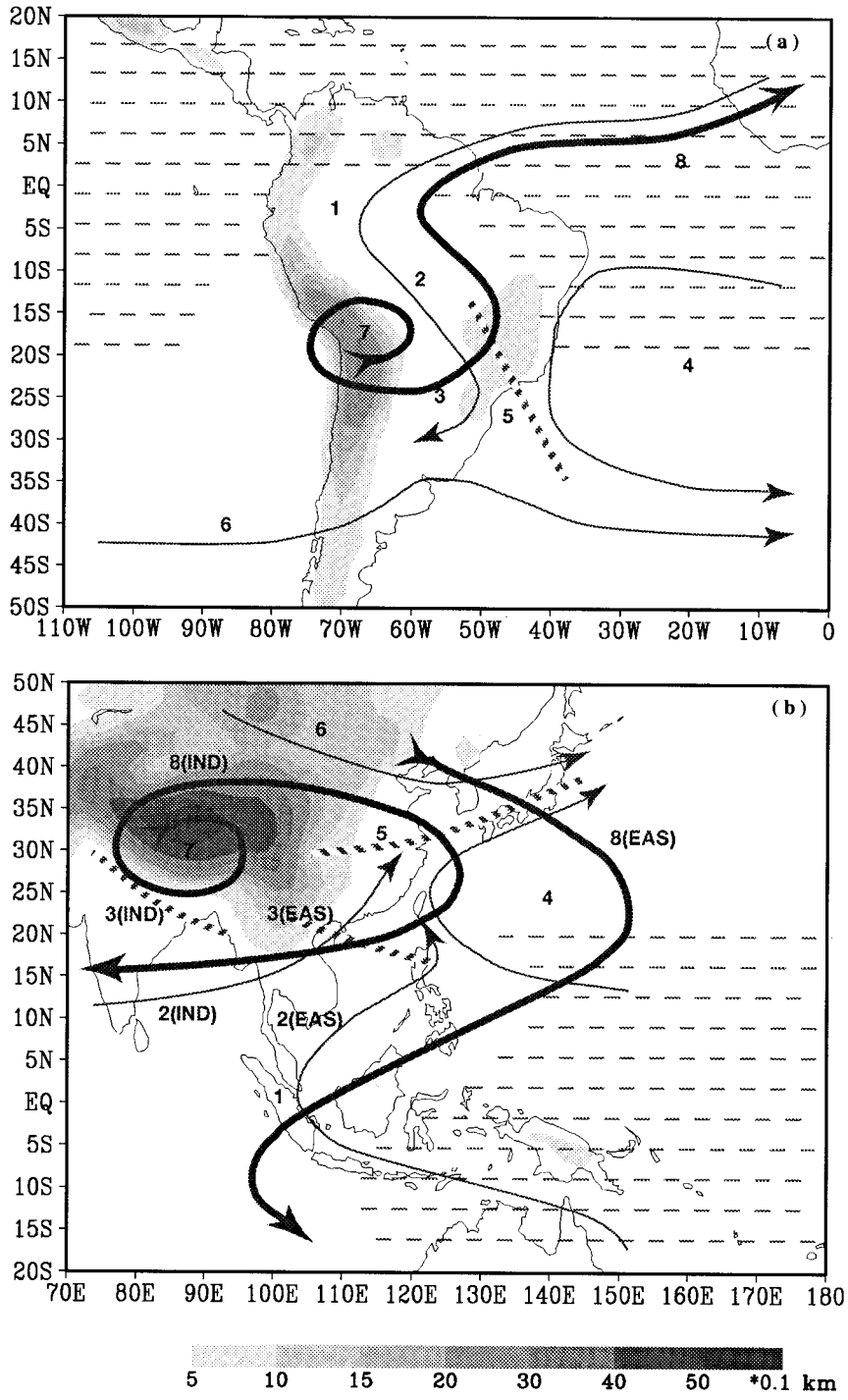

FIG. 18. Schematic illustration of elementary features for (a) SASM and (b) EASM. The shading represents the topography. The areas where easterlies prevail are indicated by dashed lines. The correspondingly numbered features are as follows: 1) low-level cross equatorial flow, 2) northwesterlies vs southwesterlies, 3) Gran Chaco low vs EASM trough, 4) subtropical high, 5) SACZ vs Mei-Yu front zone, 6) midlatitude westerlies, 7) Bolivian high vs Tibetan high, and 8) upper-level return flow.

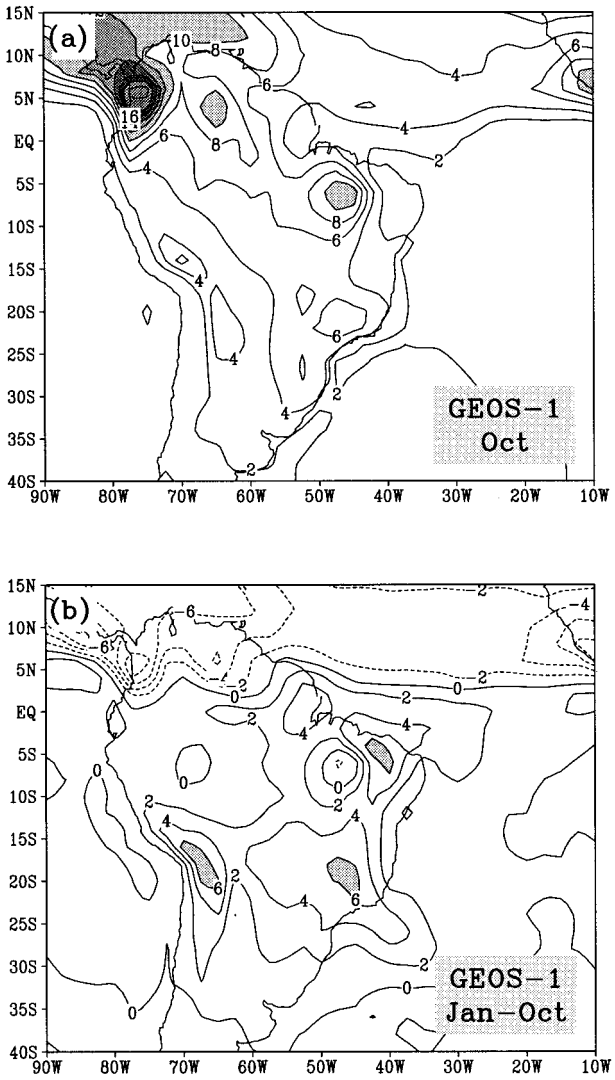

FIG. A1. Same as Fig. 1 except for the DAO climatology.

timescales is not known. These are issues that need to be addressed in future studies.

6. Concluding remarks

Using the monthly mean climatology of the GEOS-1 DAS reanalysis and comparing with NCEP reanalysis and GPI rainfall data, we have classified two circulation regimes over South America, forced by the seasonally evolving land–sea thermal contrast. In austral spring, deep convective heating dominates over Central America and the tropical Amazon basin (around 5°S). The upper-tropospheric response is in accordance with the description of linear dynamics of forced wave motion subject to weak nonlinear advection during this seasonal transition time. At the peak of austral summer (January), major diabatic heating center moves to the subtropical highland (about 20°S) along with the poleward migration of the sun. A heat low develops over Gran Chaco. Here, sharp thermal contrast between the subtropical highland and the surrounding oceans and the influence of the earth rotation are playing the role to drive the monsoon circulation. We have demonstrated that the seasonal perturbation of the low-level wind, which is superimposed on the annual mean trades, travels between the western Sahara and Gran Chaco. It is characterized by a clear reversal of its direction from winter to summer season, evidencing existence of SASM. All the major circulation features have been compared with the climatology of the NCEP reanalysis. It shows that the result we obtained is insensitive to the reanalysis scheme, indicating great climate significance.

Composite analyses show that the onset of 1989–90 SASM is signaled by the sudden change of upper-tropospheric westerlies from double maxima to a single jet. Following onset, a large-scale vortex is initiated southeast of the Altiplano Plateau and strong low-level northwesterly wind is formed along the eastern side of the tropical and subtropical Andes. At the same time, heavy precipitation occurs over southeastern Brazil. During the mature stage, SACZ and associated heavy precipitation belt shift southward about 10°. The rainfall maximum moves over the Altiplano Plateau and the circulation shows remarkable vertical wind shear between the upper- and the lower-level circulations. In a crude sense the SASM lasts about 2.5 months and withdraws with the same character but opposite sign as that of onset.

The temperature and heating evolution during the 1989–90 SASM season has also been investigated. During premonsoon phase, warming of the subtropics is confined to the lower troposphere and mainly due to the turbulent sensible heating. When the monsoon rainfall is initiated over southern Brazil hilly land, the tropospheric temperature increases significantly, creating a large temperature gradient between the subtropical highland and the South Atlantic Ocean. At this time latent heat release becomes the main heating component to maintain the thermal structure of the troposphere over the monsoon region. At the mature stage, the heating reaches its strongest and the warm air spans the widest longitudinal domain over subtropical South America. Starting from the middle of February, the heating intensity drops significantly following the equatorward migration of the sun. As a result, the east–west temperature gradient is diminished and the monsoon winds weaken eventually.

We have demonstrated an in-phase variation between the tropospheric temperature over the subtropical highland and the SASM. Such relationship is found between subtropical temperature and the tropical North Atlantic surface wind (not shown). Since SST anomaly is strongly related to anomalous surface winds, it is plausible that the tropical SST of the North Atlantic could be altered by the subtropical continental heating centered

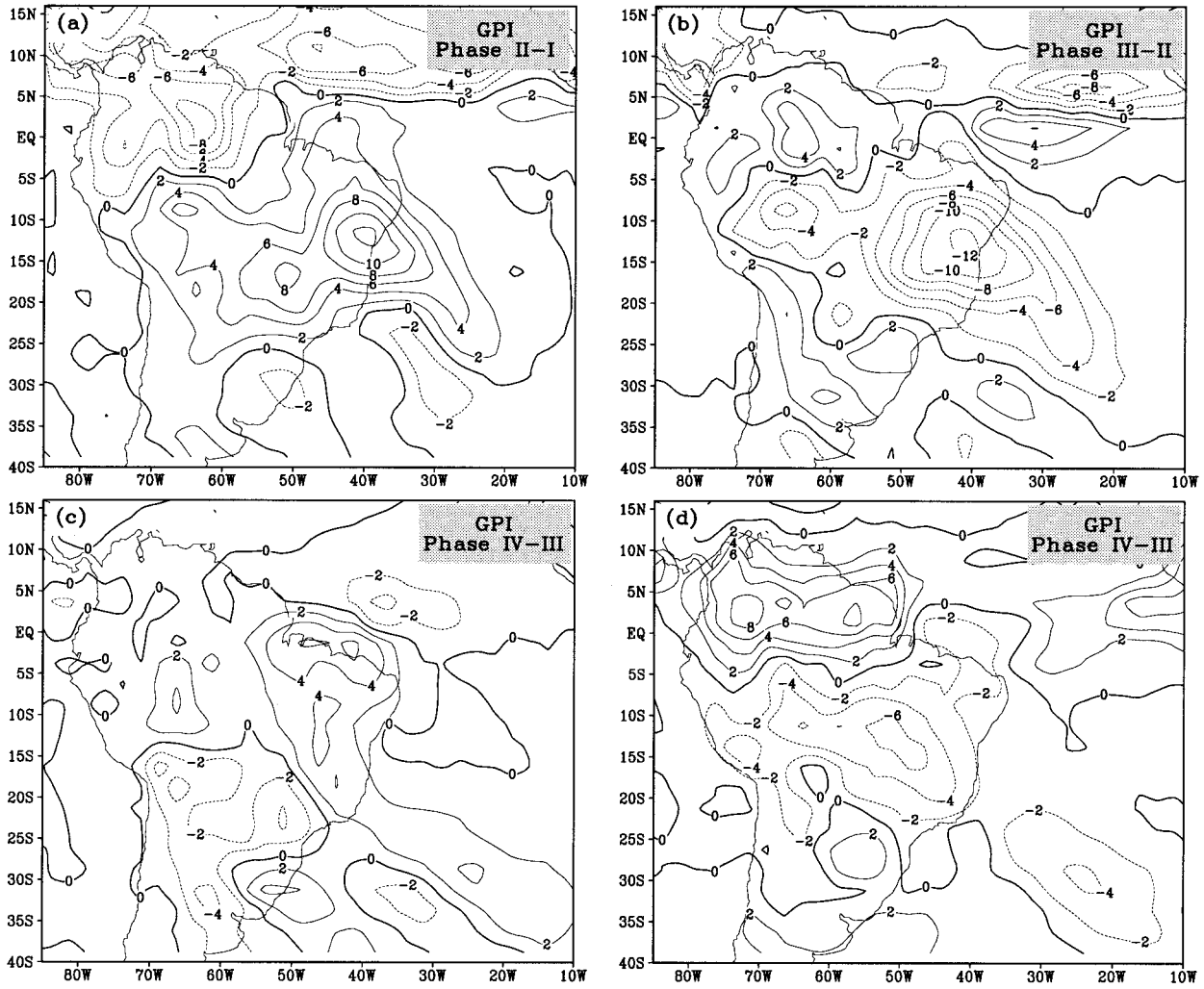

FIG. A2. Same as Fig. 13 except for the GPI estimation.

over Altiplano via the influence of SASM in the austral summertime.

We have also compared and contrasted the SASM to the classic EASM system. Several common features, including evolution characteristics between the two systems, have been identified. Contrasting features including the mechanical aspects of the Andes versus the Tibetan Plateau and the plausible different role of SASM compared to EASM in the global climate system are also discussed. Finally, we point out the important influence of the tropical surface easterlies in ''disguising'' many regional features of the SASM. When the mean easterly influence is removed, many monsoonal features become apparent. Based on the characteristic features and their evolution that we presented in this paper, we conclude that the SASM qualifies as a monsoon climate system.

Acknowledgments. Support for this research was provided by the Earth Observing System/Interdisciplinary Science investigation on hydrological processes and climate, and the Global Modeling and Analysis Program of the NASA Mission to Planet Earth Office. We thank the editor and reviewers for their constructive comments, which significantly improved this manuscript.

APPENDIX

Validation

According to several investigators (Schubert and Rood 1995; Higgins et al. 1996), large bias exists in the precipitation distribution of the GEOS and NCEP reanalyses. In our study, we used the tendency instead of the total field to reveal the character of the monsoon rainfall migration. Figures A1a and A1b show the GEOS-1 DAS precipitation climatology of the October mean and that of the difference between the January and the October mean, respectively. Compared with the October mean of GPI climatology (Fig. 1a), Fig. A1a

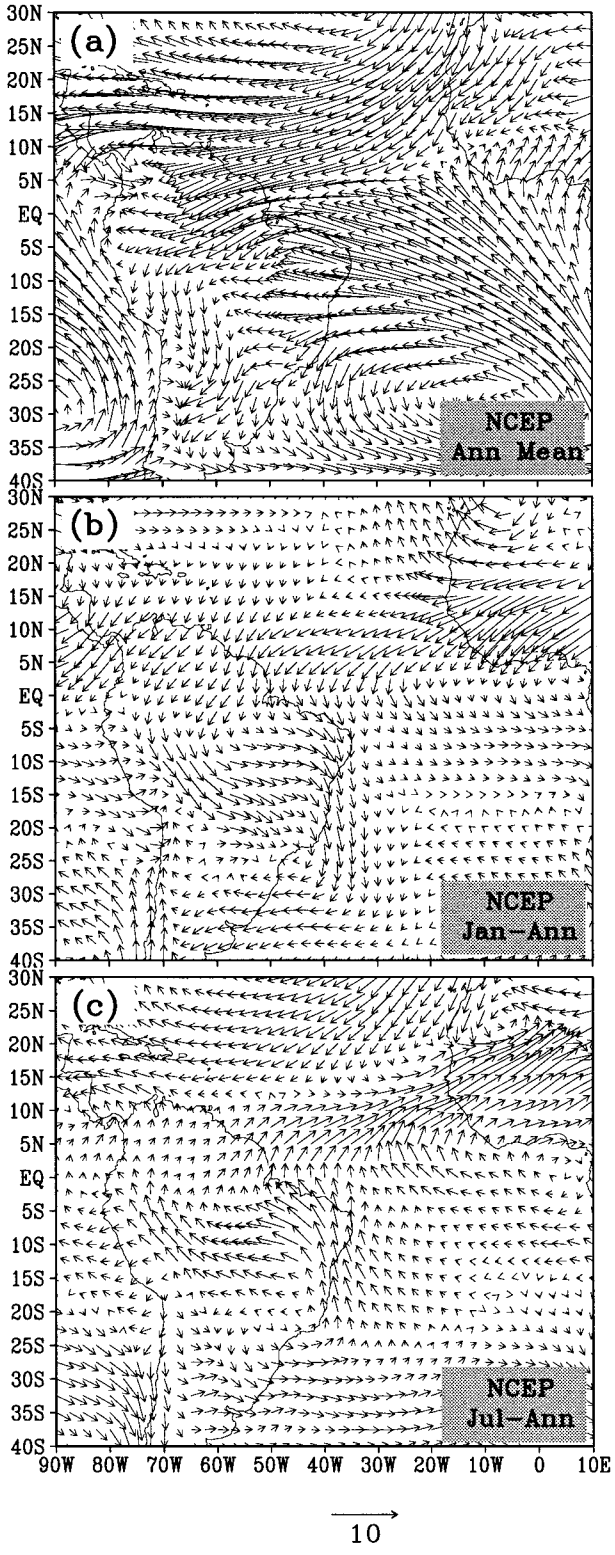

FIG. A3. Same as Fig. 9 except for the NCEP climatology of 925-hPa wind.

shows clear overestimation over the northeastern tip of South America. A heavy precipitation band, extending from Colombia to southern Brazil, swings northeastward, creating a precipitation center over northern Brazil. GEOS-1 DAS displays much weaker precipitation in the North Atlantic intertropical convergence zone (ITCZ) and a separate precipitation center over the central Andes, where only a precipitation transition zone is found in the GPI presentation. Despite these mean biases, the precipitation difference fields over the South American continent (Fig. A1b vs Fig. 1b) show much similarity between GEOS-1 DAS and GPI. Both products display the seasonal movement of heavy precipitation band from the northern Tropics to the southern subtropics. The location and the intensity of the rainfall enhancement (over the central Andes, southern Brazil, and the north coast of Brazil) are very close between the two products. The main discrepancy is found over the North Atlantic ITCZ, where GEOS-1 DAS show little variation. All these provide evidence that after removal of the systematic bias, the assimilated rainfall contains valid information. To further support our discussion on the temporal character of the SASM precipitation described in section 4b, Fig. A2 shows the GPI precipitation difference fields between successive phases of SASM as defined in the main text. Comparing Fig. A2 with Fig. 13, the spatial patterns of the corresponding phase difference are very similar. The correlations are in the range of 0.51–0.57. Major features of the monsoon rainfall movement shown in Fig. A2 were captured by Fig. 13. This approach was also recommended by other investigators (e.g., Min and Schubert 1997), who pointed out that the assimilated time mean moisture field may not be reliable, while the anomaly field, the deviation from the time mean, is much better correlated with the observation.

In section 3, we identified an anomalous low-level flow (deviation from the annual mean) from northwest Africa to Gran Chaco of central South America in January, which reverses direction in July in the GEOS-1 DAS climatology (Fig. 9). To confirm that this finding does not depend on the assimilation data used, the climatology of 925-hPa wind of the NCEP reanalysis (1979–95) is plotted in Fig. A3. Comparing with Fig. 9, the NCEP reanalysis shows stronger annual mean trade winds over the tropical Atlantic and more intense meridional flow along the west coast of South America. In July, the NCEP reanalysis gives a weaker anomalous flow along the monsoon passage. Significant southwesterlies crossing over the northern Andes as shown in the GEOS-1 assimilation is not shown in the NCEP reanalysis. Besides these differences, the overall resemblance between corresponding panels, especially for the January anomalous wind field (Fig. A3b), is clearly seen, indicating that the summer monsoon circulation is a robust climate feature of South America.

REFERENCES

Arkin, P. A., and B. N. Meisner, 1987: The relationship between large-scale convective rainfall and cold cloud cover over the western hemisphere during 1982–84. *Mon. Wea. Rev.,* **115,** 51–74.

Buchmann, J., P. L. Silva Dias, and A. D. Moura, 1986: Transient convection over the Amazon Bolivia region and the dynamics of droughts over north-east Brazil. *Arch. Meteor. Geophys. Bioklimatol.,* **34A,** 367–384.

Das, P. K., 1986: *Monsoons.* World Meteorological Organization, 155 pp.

DeMaria, M., 1985: Linear response of a stratified tropical atmosphere to convective forcing. *J. Atmos. Sci.,* **42,** 1944–1959.

Ding, Y., 1994: *Monsoons over China.* Kluwer Academic, 419 pp.

Druyan, L. M., 1981: The use of global general circulation models in the study of the Asian monsoon. *J. Climatol.,* **1,** 77–92.

Fennessy, M. J., and Coauthors, 1994: The simulated Indian monsoon: A GCM sensitivity study. *J. Climate,* **7,** 33–43.

Figueroa, S. N., P. Satyamurty, and P. L. Silva Dias, 1995: Simulations of the summer circulation over the South American region with an eta coordinate model. *J. Atmos. Sci.,* **52,** 1573–1584.

Gandu, A. W., and J. E. Geisler, 1991: A primitive equations model study of the effect of topography on the summer circulation over tropical South America. *J. Atmos. Sci.,* **48,** 1822–1836.

Gutman, G. J., and W. Schwerdtfeger, 1965: The role of latent and sensible heat for the development of a high pressure system over the subtropical Andes, in the summer. *Meteor. Rundsch.,* **18,** 69–75.

Hahn, D. G., and S. Manabe, 1975: The role of mountains in the south Asian monsoon circulation. *J. Atmos. Sci.,* **32,** 1515–1541.

Halley, E., 1686: An historical account of the trade winds and monsoons observable in the seas between and near the tropics, with an attempt to assign the physical cause of the winds. *Philos. Trans. Roy. Soc. London,* **26,** 153–168.

He, H., J. W. McGinnis, Z. Song, and M. Yanai, 1987: Onset of the Asian summer monsoon in 1979 and the effect of the Tibetan Plateau. *Mon. Wea. Rev.,* **115,** 1966–1995.

Higgins, R. W., Y. Yao, M. Chelliah, W. Ebisuzaki, J. E. Janowiak, C. F. Ropelewski, and R. E. Kistler, 1996: Intercomparison of the NCEP/NCAR and the NASA/DAO reanalysis (1985–1993). NCEP/Climate Prediction Center Atlas No. 2, U.S. Department of Commerce, National Oceanic and Atmospheric Administration, and National Weather Service, 169 pp.

Joshi, P. C., B. Simon, and P. S. Desai, 1990: Atmospheric thermal changes over the Indian region prior to the monsoon onset as observed by satellite sounding data. *Int. J. Climatol.,* **10,** 49–56.

Kalnay, E., K. C. Mo, and J. Paegle, 1986: Large-amplitude, short-scale stationary Rossby waves in the Southern Hemisphere: Observations and mechanistic experiments to determine their origin. *J. Atmos. Sci.,* **43,** 252–275.

——, and Coauthors, 1996: The NCEP/NCAR 40-year reanalysis project. *Bull. Amer. Meteor. Soc.,* **77,** 437–471.

Khromov, S. P., 1957: Die geographische Verbreitung der Monsune. *Petermanns Geogr.,* **101,** 234–237.

Kleeman, R., 1989: A modeling study of the effect of the Andes on the summertime circulation of tropical South America. *J. Atmos. Sci.,* **46,** 3344–3362.

Kodama, Y., 1992: Large-scale common features of subtropical precipitation zones (the Baiu frontal zone, the SPCZ, and the SACZ). Part I: Characteristics of subtropical frontal zones. *J. Meteor. Soc. Japan,* **70,** 813–835.

Kousky, V. E., and M. Alonso Gan, 1981: Upper-tropospheric cyclonic vortices in the tropical South Atlantic. *Tellus,* **33,** 538–551.

Krishnamurti, T. N., and H. N. Bhalme, 1976: Oscillations of a monsoon system. Part I: Observational aspects. *J. Atmos. Sci.,* **33,** 1937–1953.

——, and D. Subrahmanyam, 1982: The 30–50 day mode at 850 mb during MONEX. *J. Atmos. Sci.,* **39,** 2088–2095.

Lau, K.-M., 1992: East Asian summer rainfall variability and climate teleconnection. *J. Meteor. Soc. Japan,* **70,** 211–242.

——, and M.-T. Li, 1984: The monsoon of east Asia and its global associations—A survey. *Bull. Amer. Meteor. Soc.,* **65,** 114–125.

——, G. J. Yang, and S. H. Shen, 1988: Seasonal and intraseasonal climatology of summer monsoon rainfall over east Asia. *Mon. Wea. Rev.,* **116,** 18–37.

Lenters, J. D., and K. H. Cook, 1995: Simulation and diagnosis of the regional summertime precipitation climatology of South America. *J. Climate,* **8,** 2988–3005.

Luo, H., and M. Yanai, 1984: The large-scale circulation and heat sources over the Tibetan Plateau and surrounding areas during the early summer of 1979. Part II: Heat and moisture budgets. *Mon. Wea. Rev.,* **112,** 966–989.

Meehl, G. A., 1993: A coupled air–sea biennial mechanism in the tropical Indian and Pacific regions: Role of the ocean. *J. Climate,* **6,** 31–41.

Min, W., and S. Schubert, 1997: The climate signal in regional moisture fluxes: A comparison of three global data assimilation products. *J. Climate,* **10,** 2623–2642.

Ramage, C. S., 1971: *Monsoon Meteorology.* Academic Press, 269 pp.

Rao, G. V., and S. Erdogan, 1989: The atmospheric heat source over the Bolivian Plateau for a mean January. *Bound.-Layer Meteor.,* **46,** 13–33.

Schubert, S. D., and R. Rood, 1995: Proceedings of the workshop on the GEOS-1 five year assimilation. Vol. 7, Tech. Rep. Series on Global Modeling and Data Assimilation, NASA Tech. Memo. 104606, 201 pp. [Available from Data Assimilation Office, NASA/Goddard Space Flight Center, Greenbelt, MD 20771.]

——, J. Pfaendtner, and R. Rood, 1993: An assimilated dataset for earth science applications. *Bull. Amer. Meteor. Soc.,* **74,** 2331–2342.

Schwerdtfeger, W., 1961: Stromungs- und Temperaturfeld der freien Atmosphäre über den Anden. *Meteor. Rundsch.,* **14,** 1–6.

Shen, S., and K.-M. Lau, 1995: Biennial oscillation associated with the east Asian summer monsoon and tropical sea surface temperatures. *J. Meteor. Soc. Japan,* **73,** 105–124.

Silva Dias, P. L., W. H. Schubert, and M. DeMaria, 1983: Large-scale response of the tropical atmosphere to transient convection. *J. Atmos. Sci.,* **40,** 2689–2707.

——, J. P. Bonatti, and V. E. Kousky, 1987: Diurnally forced tropical tropospheric circulation over South America. *Mon. Wea. Rev.,* **115,** 1465–1478.

Tao, S., and L. Chen, 1987: A review of recent research on the east Asian summer monsoon in China. *Monsoon Meteorology,* C.-P. Chang and T. N. Krishnamurti, Eds., Oxford University Press, 60–92.

van Loon, H., 1972: Wind in the Southern Hemisphere. *Meteorology of the Southern Hemisphere,* C. W. Newton, Ed., Amer. Meteor. Soc., 87–100.

Virji, H., 1981: A preliminary study of summertime tropospheric circulation patterns over South America estimated from cloud winds. *Mon. Wea. Rev.,* **109,** 599–610.

Webster, P. J., and S. Yang, 1992: Monsoon and ENSO: Selectively interactive systems. *Quart. J. Roy. Meteor. Soc.,* **118,** 877–926.

Xie, P., and P. A. Arkin, 1995: An intercomparison of gauge observations and satellite estimates of monthly precipitation. *J. Appl. Meteor.,* **34,** 1143–1160.

Yanai, M., S. Esbensen, and J.-H. Chu, 1973: Determination of bulk properties of tropical cloud clusters from large-scale heat and moisture budgets. *J. Atmos. Sci.,* **30,** 611–627.

Ye, D., 1981: Some characteristics of the summer circulation over the Qinghai-Xizang (Tibet) Plateau and its neighborhood. *Bull. Amer. Meteor. Soc.,* **62,** 14–19.

Zhou, J., Y. C. Sud, and K.-M. Lau, 1996: Impact of orographically induced gravity-wave drag in the GLA GCM. *Quart. J. Roy. Meteor. Soc.,* **122,** 903–927.